Journal of Mathematical Biology (2022) 85:47
https://doi.org/10.1007/s00285-022-01817-0

Mathematical Biology

Maximal total population of species in a diffusive logistic model

Chiu-Yen Kao[1] · Seyyed Abbas Mohammadi[2]

Received: 11 October 2021 / Revised: 7 July 2022 / Accepted: 26 September 2022 /
Published online: 7 October 2022

Abstract

In this paper, we investigate the maximization of the total population of a single species which is governed by a stationary diffusive logistic equation with a fixed amount of resources. For large diffusivity, qualitative properties of the maximizers like symmetry will be addressed. Our results are in line with previous findings which assert that for large diffusion, concentrated resources are favorable for maximizing the total population. Then, an optimality condition for the maximizer is derived based upon rearrangement theory. We develop an efficient numerical algorithm applicable to domains with different geometries in order to compute the maximizer. It is established that the algorithm is convergent. Our numerical simulations give a real insight into the qualitative properties of the maximizer and also lead us to some conjectures about the maximizer.

Keywords Diffusive logistic equation · Optimal control · Population dynamics · Rearrangements · Gradient-based algorithm

Mathematics Subject Classification 49K20 · 35Q92 · 49J30 · 49M05

✉ Chiu-Yen Kao
Chiu-Yen.Kao@claremontmckenna.edu

Seyyed Abbas Mohammadi
abbas.mohammadi@wits.ac.za

1 Department of Mathematical Sciences, Claremont McKenna College, 850 Columbia Ave, Claremont, CA 91711, USA

2 School of Computer Science and Applied Mathematics, University of The Witwatersrand, 1 Jan Smuts Avenue, Braamfontein, Johannesburg, Gauteng 2000, South Africa

1 Introduction

Spatially heterogeneous models are of great importance in conservation biology (Goss-Custard et al. 2003). Considering such models, there are some natural questions to be addressed. Existence, uniqueness and stability of equilibriums for heterogeneous systems of reaction–diffusion equations are some of such questions, see for instance He and Ni (2017), Yousefnezhad and Mohammadi (2016), and Yousefnezhad et al. (2018). Recently, the question of maximizing the total population size has drawn considerable attention from both mathematical and biological fields since the population abundance is clearly a good measurement for the conservation of a single species (Ding et al. 2010; Mazari et al. 2020; Mazari and Ruiz-Balet 2021; Nagahara and Yanagida 2018).

In this paper an optimal control problem is studied to maximize the total population of a single species. We consider the following semilinear elliptic equation

$$\begin{cases} \mu \Delta u + m(\mathbf{x})\, u - u^2 = 0 & \text{in } \Omega, \\ \frac{\partial u}{\partial \mathbf{n}} = 0 & \text{on } \partial\Omega, \end{cases} \tag{1}$$

where $\mu > 0$, $m(\mathbf{x}) \in L^\infty(\Omega)$ is a non-negative, non-zero function, Ω is a bounded domain in $\mathbb{R}^N$ with smooth boundary $\partial\Omega$ and $\mathbf{n}$ is the outward unit normal vector on the boundary.

It is well known that Eq. (1) has a unique positive solution $u(\mathbf{x}) = u_{\mu,m}(\mathbf{x})$ in $W^{2,p}(\Omega) \cap C^{1,\alpha}(\bar{\Omega})$ for $\alpha \in (0, 1)$ and $p > 1$. Also, we know that

$$0 < \inf_{\bar{\Omega}} u \leq u \leq \|m\|_{L^\infty(\Omega)}, \tag{2}$$

see Berestycki et al. (2005), Ding et al. (2010), Mazari et al. (2020), and Nagahara and Yanagida (2018).

Problem (1) arises as a stationary equation of a reaction–diffusion PDE modeling the growth of biological populations and plays an important role in studying the effects of dispersal and spatial heterogeneity in population dynamics (Cantrell and Cosner 1989, 1991; Skellam 1951). From a biological point of view, Ω is the habitat of a species and the zero-flux boundary condition in (1) accounts for the fact that no individuals cross the boundary of the habitat. The function $m(\mathbf{x})$ stands for the intrinsic growth rate of the species at location $\mathbf{x}$ which in a way can be considered as a measure of the resources available at $\mathbf{x}$. The set $\{\mathbf{x} \mid m(\mathbf{x}) > 0\}$ corresponds to the place in the habitat which is favorable to the species since resources are available there. The parameter μ represents the dispersal ability of the species or the diffusion rate.

It was observed by Lou (2006) that

$$\int_\Omega m(\mathbf{x}) d\mathbf{x} < \int_\Omega u_{\mu,m}(\mathbf{x}) d\mathbf{x}, \tag{3}$$

which implies that a total population at equilibrium is greater than the total carrying capacity in a spatially heterogeneous environment. It was conjectured by Ni that, among all spatial distributions of resources and the dispersal rate, μ, the ratio of the total population at equilibrium and the total carry capacity is bounded from above by 3, and that the constant is sharp in one dimension. This conjecture was later proved in Bai et al. (2016).

We are interested in investigating how the allocation of resources influences the population size of the species. Therefore, we consider the following optimization problem. For $A \in (0, |\Omega|)$ define

$$\mathcal{M} = \left\{ m \in L^\infty(\Omega) : \; 0 \le m(\mathbf{x}) \le 1, \; \int_\Omega m(\mathbf{x}) d\mathbf{x} = A \right\},$$

and our objective functional

$$J(m) = \int_\Omega u_{\mu,m}(\mathbf{x}) d\mathbf{x}.$$

We want to determine $\hat{m} \in \mathcal{M}$ such that

$$J^\star = J(\hat{m}) = \max_{m \in \mathcal{M}} \; J(m). \tag{4}$$

The integral $\int_\Omega m(\mathbf{x}) d\mathbf{x}$ represents the total amount of resources and $J(m)$ denotes the total population of the species. The functional $J(m)$ can be considered as a good measurement for the conservation of a single species and also plays an important role in preventing the invasion of alien species (Lou 2006). Indeed, in the optimization problem (4), we want to maximize the total population size of the species while we have a fixed amount of resources. If we distribute the resources in the habitat with the optimal resource $\hat{m}$, then the resident species has the highest population size, with a given resource amount A, and so usually it is harder for other species to invade its habitat. Similar questions regarding the optimal allocation of resources have also been investigated in the framework of eigenvalue problems (Chugunova et al. 2016; Cosner et al. 2013; Hintermüller et al. 2012; Kao et al. 2008; Lamboley et al. 2016; Lou 2008; Lou and Yanagida 2006).

It has been established that problem (1) admits a solution by using a standard variational method (Ding et al. 2010). At the mathematical level, it is hard and challenging to deal with the nonenergetic functional $J(m)$ to derive qualitative properties of the maximizer since the structure of the functional and boundary conditions in (1) avoid employing classical tools (e.g., rearrangements, symmetrization). The main challenging qualitative question corresponding to this optimization problem was whether the maximizer $\hat{m}$ is of bang-bang type, i.e., there exists a set $\hat{D} \subset \Omega$ with $|\hat{D}| = A$ such that $\hat{m} = \chi_{\hat{D}}$. Having a bang-bang type maximizer yields $\hat{m} = \chi_{\hat{D}}$ and the maximization problem (4) can be recast in terms of the following shape optimization problem

$$J(\hat{m}) = \max_{m \in \mathcal{N}} J(m), \tag{5}$$

where $\mathcal{N} = \{\chi_D : \; D \subset \Omega, \; |D| = A\}$. This implies that with limited resources, one should put all the resources in some suitable set $\hat{D}$, a protected area, in order to maximize the total population size. Numerical simulations in Ding et al. (2010), Mazari and Ruiz-Balet (2021) supported the conjecture that the maximizers of (4) are of bang-bang type. It has been proved that all local maximizers $\hat{m}$ of (4) that are Riemann integrable are of bang–bang type (Nagahara and Yanagida 2018). Moreover, the same result has been obtained in Mazari et al. (2020) assuming large diffusivity. Recently this question was settled by Mazari et al. (2021) and it has been established that the maximizers of (4) are of bang-bang type regardless of the value of $\mu > 0$. One can see the discussion on a more general model in Lam et al. (2020) which accounts for spatial dependent intrinsic growth rate and carrying capacity.

In this paper, after providing preliminaries in Sect. 2, we aim at obtaining qualitative properties of the maximizer for a large diffusivity in Sect. 3. Considering N-balls and annuli, our results suggest that symmetric properties or even radial structure for the maximizers of (4) may hold while $\mu \to \infty$. These qualitative properties are in line with results in Mazari et al. (2020), Mazari and Ruiz-Balet (2021) which assert that for large diffusion, concentrated resources are favorable for maximizing the total population. In Sect. 4, an optimality condition for the maximizer of (4) is obtained based upon rearrangement theory. From both mathematical and biological point of view, it is a natural question to know about the shape of the optimal set $\hat{D}$ and thus it is necessary to have a numerical method to determine a solution for (4). We develop a gradient-based numerical algorithm to compute the maximizer invoking rearrangement techniques. The convergence of the algorithm is investigated. Our numerical algorithm is efficient and applicable for domains with different geometries and the numerical results validate our findings and also theoretical results in Ding et al. (2010), Mazari et al. (2020, 2021), Mazari and Ruiz-Balet (2021), Nagahara and Yanagida (2018), and Heo and Kim (2021). With an eye on the biological interpretations, numerical results give a real insight into the qualitative properties of the maximizer, in particular for the challenging case of small diffusions, and also lead us to some conjectures about the maximizer which are stated in the conclusion section.

2 Preliminaries

In this section we provide some basic and well-known results about rearrangement theory (Burton 1987, 1989) that will be required in our analysis.

Two Lebesgue measurable functions $f : \Omega \to \mathbb{R}$, $\tilde{f} : \Omega \to \mathbb{R}$, are said to be rearrangements of each other if

$$|\{\mathbf{x} \in \Omega : f(\mathbf{x}) \geq \theta\}| = |\{\mathbf{x} \in \Omega : \tilde{f}(\mathbf{x}) \geq \theta\}| \qquad \forall \theta \in \mathbb{R}. \tag{6}$$

The set of functions which are rearrangement of $\tilde{f}$ is called the rearrangement class generated by $\tilde{f}$. Considering $\tilde{f} = \chi_{\tilde{D}}$ with $|\tilde{D}| = A$, it is easy to check that all functions in $\mathcal{N}$ are rearrangements of $\tilde{f}$ and indeed $\mathcal{N} \subset L^2(\Omega)$ is the rearrangement class generated by this function. It is well known that the weak closure of this set in $L^2(\Omega)$ is $\mathcal{M}$ which has the following properties, see Burton (1989, Lemmas 2.2 and 2.3).

Lemma 1 *The set $\mathcal{M}$ is convex and weakly sequentially compact. Moreover, $\mathcal{N}$ is the set of extreme points of $\mathcal{M}$.*

We need the following technical result.

Lemma 2 *Consider h in $\mathcal{M}\backslash\mathcal{N}$ and η in $\mathcal{N}$. Then we have $\|h\|_{L^2(\Omega)} \leq \|\eta\|_{L^2(\Omega)}$.*

Proof Since $\mathcal{M}$ is the weak closure of $\mathcal{N}$, there is sequence $\{f_i\}_1^\infty \subset \mathcal{N}$ such that $f_i \rightharpoonup h$ in $L^2(\Omega)$. It is easy to check that the L^2-norm of all functions in $\mathcal{N}$ equals to $\sqrt{A}$. Employing the weak lower semi-continuity of the norm, we have

$$\|h\|_{L^2(\Omega)} \leq \liminf_{i\to\infty} \|f_i\|_{L^2(\Omega)} = \sqrt{A} = \|\eta\|_{L^2(\Omega)}.$$

□

Here we provide a brief introduction of cap or spherical symmetrization (Sperner 1981; Brock 2007). Hereafter $B(\mathbf{0}, r)$ represents an open ball centered at the origin with radius r. Given a unit vector $\mathbf{e}$ as the direction, consider a measurable set $D \subset \mathbb{R}^N$. Then, the cap symmetrization of D with respect to direction $\mathbf{e}$, denoted by D^*, is defined in the following way: for all $r \in (0, \infty)$, the set $D^* \cap \partial B(\mathbf{0}, r)$ is a spherical cap centered at $r\mathbf{e}$ satisfying

$$\mathcal{H}^{N-1}(D^* \cap \partial B(\mathbf{0}, r)) = \mathcal{H}^{N-1}(D \cap \partial B(\mathbf{0}, r)), \quad \text{for all} \quad r > 0,$$

where $\mathcal{H}^{N-1}$ denotes the $(N-1)$-dimensional Hausdorff measure in $\mathbb{R}^N$. For a measurable function v, the cap symmetrization v^* is a rearrangement of v such that

$$\{\mathbf{x} \in \Omega : v^*(\mathbf{x}) \geq \theta\} = \{\mathbf{x} \in \Omega : v(\mathbf{x}) \geq \theta\}^*, \quad \text{for all} \quad \theta > 0,$$

see Sperner (1981, Page 1) or Brock (2007, Sect. 3.3). In order to determine nearly optimal solutions, we need the following result about cap symmetrization, see Brock (2007, Theorem 4.5).

Lemma 3 *Let $v \in H^1(\Omega)$ where either $\Omega = B(\mathbf{0}, r)$ or $\Omega = B(\mathbf{0}, r_2)\backslash\overline{B(\mathbf{0}, r_1)}$ for some $r_2 > r_1 \geq 0$. Then, we have $v^* \in H^1(\Omega)$ and $\|\nabla v\|_{L^2(\Omega)} \geq \|\nabla v^*\|_{L^2(\Omega)}$.*

The following result is attributed to Hardy et al. (1952, Chapter 10).

Lemma 4 *Consider $u, v \in L^2(\Omega)$ where either $\Omega = B(\mathbf{0}, r)$ or $\Omega = B(\mathbf{0}, r_2)\backslash\overline{B(\mathbf{0}, r_1)}$ for some $r_2 > r_1 \geq 0$. Then, we have*

$$\int_\Omega uv d\mathbf{x} \leq \int_\Omega u^* v^* d\mathbf{x}.$$

The following lemma which is a modification of the bathtub principle is required.

Lemma 5 *Consider $f(\mathbf{x}) \in L^1(\Omega)$. Then the maximization problem*

$$\max_{m \in \mathcal{M}} \int_\Omega m(\mathbf{x}) f(\mathbf{x}) d\mathbf{x},$$

is solvable by $m(\mathbf{x}) = \chi_D$ such that $|D| = A$ and

$$\{\mathbf{x} \in \Omega : \ f(\mathbf{x}) > t\} \subset D \subset \{\mathbf{x} \in \Omega : \ f(\mathbf{x}) \geq t\}, \tag{7}$$

where

$$t = \sup\{s \in \mathbb{R} : \ |\{\mathbf{x} \in \Omega : \ f(\mathbf{x}) \geq s\}| \geq A\}. \tag{8}$$

Moreover, this solution is unique if set $\{\mathbf{x} \in \Omega : \ f(\mathbf{x}) = t\}$ has zero Lebesgue measure and we have $D = \{\mathbf{x} \in \Omega : \ f(\mathbf{x}) \geq t\}$.

Proof Considering the fact that

$$\max_{m \in \mathcal{M}} \int_\Omega m(\mathbf{x}) f(\mathbf{x}) d\mathbf{x} = - \min_{m \in \mathcal{M}} \int_\Omega m(\mathbf{x})(-f(\mathbf{x})) d\mathbf{x},$$

the assertion is obtained in view of Lieb and Loss (2001, Theorem 1.14). □

3 Nearly optimal solution

This section is devoted to nearly optimal solutions when the diffusion is large. A nearly optimal solution is a function $m \in \mathcal{M}$ which is in good agreement with the maximizer of (4) when μ is large enough. Denote $\tau = A/|\Omega|$. It is known that $u \to \tau$ when $\mu \to \infty$ (Lou 2006). Following the idea in He and Ni (2016a, b, 2017), and Mazari et al. (2020), when μ is large, there is a function v such that

$$u \approx \tau + \frac{v + \frac{1}{\tau^2 |\Omega|} \int_\Omega |\nabla v|^2 d\mathbf{x}}{\mu}.$$

Given $m \in L^2(\Omega)$ with $\int_\Omega m d\mathbf{x} = A$, v satisfies the following boundary value problem

$$\begin{cases} \Delta v = \tau(\tau - m) & \text{in } \Omega, \\ \frac{\partial v}{\partial \mathbf{n}} = 0 & \text{on } \partial\Omega, \\ \int_\Omega v d\mathbf{x} = 0, \end{cases} \tag{9}$$

where $\tau = A/|\Omega|$. This equation has a non-trivial solution (Mazari et al. 2020) and the uniqueness is ensured by the integral constraint. Moreover, the solution belongs to $H^2(\Omega) \cap C^{1,\alpha}(\Omega)$ for some $\alpha > 0$, see Gilbarg and Trudinger (2015, Theorem 8.8) and Lê (2006, Theorem 4.4). It is well known that $v = v_m(\mathbf{x})$ satisfies (9) if it is a solution of the following maximization problem

$$\sup_{v \in H^1(\Omega),\ \int_\Omega v d\mathbf{x} = 0} 2\tau \int_\Omega m v d\mathbf{x} - \int_\Omega |\nabla v|^2 d\mathbf{x},$$

and then in view of the integral constraint in (9) we have

$$\int_\Omega |\nabla v_m|^2 d\mathbf{x} = \tau \int_\Omega m v_m d\mathbf{x},$$

for the maximizer. Let $\mathcal{F}(m) = \int_\Omega |\nabla v_m|^2 d\mathbf{x}$ and consider the following maximization problem

$$\sup_{m \in \mathcal{M}} \mathcal{F}(m). \tag{10}$$

It has been proved that (10) has a solution $\tilde{m} = \chi_{\tilde{D}}$ in view of the fact that $\mathcal{F}(m)$ is a strictly convex functional (Mazari et al. 2020). The maximizer of (10) is a nearly optimal solution of (4). This means that when $\mu \to \infty$ the family $\{\hat{m}_\mu\}_{\mu>0}$ which are solutions of (4) corresponding to μ, converges up to a subsequence to a solution of (10) in $L^1(\Omega)$, see Mazari et al. (2020, Theorem 2).

Lemma 6 *Let $m \in \mathcal{M}$ and assume that $N < 4$. The functional $\mathcal{F}$ is Gateaux differentiable at m and we have*

$$(\mathcal{F}'(m), h) = 2\tau \int_\Omega h v_m d\mathbf{x},$$

for all $h \in L^2(\Omega)$ with $\int_\Omega h d\mathbf{x} = 0$.

Proof Setting $v_t = v_{m+th} - v_m$, it is easy to check that v_t satisfies

$$\begin{cases} \Delta v_t = -t\tau h & \text{in } \Omega, \\ \frac{\partial v_t}{\partial \mathbf{n}} = 0 & \text{on } \partial\Omega, \\ \int_\Omega v_t d\mathbf{x} = 0. \end{cases} \tag{11}$$

Using Sobolev embeddings and regularity results for elliptic equations, Gilbarg and Trudinger (2015, Theorem 8.8), we obtain

$$\begin{aligned} \|v_t\|_{C(\bar{\Omega})} \leq C_1 \|v_t\|_{H^2(\Omega)} &\leq C_2 \left(\|v_t\|_{H^1(\Omega)} + t\tau \|h\|_{L^2(\Omega)}\right) \\ &\leq C_2 t\tau \|h\|_{L^2(\Omega)} \left(\|v_t\|_{L^2(\Omega)} + 1\right), \end{aligned}$$

which yields that $v_{m+th} \to v_m$ uniformly as $t \to 0$. On the other-hand, it is easy to check that for all m, n in $L^2(\Omega)$, we have

$$\int_\Omega n v_m d\mathbf{x} = \int_\Omega m v_n d\mathbf{x}, \tag{12}$$

in view of the fact that v_m and v_n are solutions of (9) corresponding to m and n respectively.

Using these findings, it is inferred that

$$
\begin{aligned}
(\mathcal{F}'(m), h) &= \tau \lim_{t\to 0} \frac{\int_\Omega (m+th)v_{m+th}d\mathbf{x} - \int_\Omega m v_m d\mathbf{x}}{t}\\
&= \tau \lim_{t\to 0} \frac{\int_\Omega m v_m d\mathbf{x} + t\int_\Omega h v_m d\mathbf{x} + t\int_\Omega h v_{m+th} d\mathbf{x} - \int_\Omega m v_m d\mathbf{x}}{t}\\
&= 2\tau \int_\Omega h v_m d\mathbf{x},
\end{aligned}
$$

in view of (12) and the fact that $v_{m+th} \to v_m$ uniformly as $t \to 0$. □

The following lemma provides an optimality condition for a local maximizer of (10). Let $B(m, \epsilon)$ be a ball in $L^2(\Omega)$ centered at m with radius $\epsilon > 0$. Then, $\tilde{m}$ is a local maximizer for (10) if there exists an $\epsilon > 0$ such that

$$
\mathcal{F}(\tilde{m}) \geq \mathcal{F}(m) \quad \text{for all} \quad m \in B(\tilde{m}, \epsilon) \cap \mathcal{M}.
$$

Lemma 7 *Assume that $\tilde{m} = \chi_{\tilde{D}}$ is a local maximizer of (10) and $N < 4$. Then, we have*

$$
\int_\Omega \tilde{m} v_{\tilde{m}} d\mathbf{x} \geq \int_\Omega h v_{\tilde{m}} d\mathbf{x}, \quad \textit{for every} \quad h \in \mathcal{M}.
$$

Moreover, there is a non-decreasing function $\phi : \mathbb{R} \to \mathbb{R}$ such that $\tilde{m} = \phi(v_{\tilde{m}})$ and also $\tilde{D}$ is uniquely determined in the following form

$$
\tilde{D} = \{\mathbf{x} \in \Omega : \ v_{\tilde{m}} \geq \tilde{t}\}, \quad \textit{such that} \quad \tilde{t} = \sup\{s : |\{\mathbf{x} \in \Omega : v_{\tilde{m}} \geq s\}| \geq A\}.
$$

Proof Consider $h \in \mathcal{M}$, then in view of Lemma 1 we know that $\tilde{m} + t(h - \tilde{m})$ belongs to $\mathcal{M}$ for $t \in (0, 1)$. Now, Lemma 6 yields

$$
2\tau \int_\Omega (h - \tilde{m}) v_{\tilde{m}} d\mathbf{x} = \lim_{t\to 0^+} \frac{\mathcal{F}(\tilde{m} + t(h - \tilde{m})) - \mathcal{F}(\tilde{m})}{t} \leq 0,
$$

and so

$$
\int_\Omega \tilde{m} v_{\tilde{m}} d\mathbf{x} \geq \int_\Omega h v_{\tilde{m}} d\mathbf{x}, \quad \text{for every} \quad h \in \mathcal{M}.
$$

The last inequality says that $\tilde{m}$ is a maximizer of the functional $L(h) = \int_\Omega h v_{\tilde{m}} d\mathbf{x}$ over $\mathcal{M}$. In view of (9), we know that $\Delta v_{\tilde{m}} = \tau^2 - \tau\chi_{\tilde{D}}$ almost everywhere in Ω. Since $\tau = \frac{A}{|\Omega|} < 1$, it is inferred that $\Delta v_{\tilde{m}} < 0$ almost everywhere in $\tilde{D}$ and $\Delta v_{\tilde{m}} > 0$ otherwise. Using Lemma 7.7 in Gilbarg and Trudinger (2015), it is concluded that the graph of $v_{\tilde{m}}$ has no significant flat section. Now employing Lemmas 2.4 and 2.9 in Burton (1989), it is deduced that there is a non-decreasing function ϕ such that $\phi(v_{\tilde{m}})$

is the unique maximizer of $L(h)$. Consequently, we have $\tilde{m} = \chi_{\tilde{D}} = \phi(v_{\tilde{m}})$. Then, it is inferred that there is $\tilde{t}$ such that $\phi(s) = 0$ for $s < \tilde{t}$ and $\phi(s) = 1$ for $s \geq \tilde{t}$ where

$$\tilde{D} = \{\mathbf{x} \in \Omega : \ v_{\tilde{m}} \geq \tilde{t}\}, \quad \text{such that} \quad \tilde{t} = \sup\{s : |\{\mathbf{x} \in \Omega : v_{\tilde{m}} \geq s\}| \geq A\},$$

due to $|\tilde{D}| = A$. □

The following theorem reveals that (10) has a cap symmetric solution $m^* = \chi_{D^*}$ in balls or annuli. For instance let $\mathbf{e} = (1, 0, .., 0) \in \mathbb{R}^N$, this means that D^* consists of spherical caps centered at $\mathbf{e}$. Indeed, if $D^* \subset \mathbb{R}^2$ in polar coordinates $r \geq 0$ and $\theta_1 \in [-\pi, \pi]$, D^* is symmetric in θ_1, convex in θ_1 and concentrated about the positive x_1−axis. Moreover, v_{D^*} on D^* depends only on the radial distance $r = \|\mathbf{x}\|$ and on the geographical latitude $\theta_1 := \arccos(x_1/\|\mathbf{x}\|)$, and is non-increasing in $\theta_1 \in [0, \pi]$ (Brock 2007; Kawohl 2006).

Theorem 1 *Let Ω be ball $B(\mathbf{0}, r_2)$ or annulus $B(\mathbf{0}, r_2)\backslash\overline{B(\mathbf{0}, r_1)}$ for some $r_2 > r_1 \geq 0$ and $\mathbf{e}$ be an arbitrary direction. Then problem (10) has a cap symmetric solution $m^* = \chi_{D^*}$ with respect to $\mathbf{e}$.*

Proof Fix $m \in \mathcal{M}$. Recall that $\int_\Omega |\nabla v_m|^2 d\mathbf{x} = \tau \int_\Omega m v_m d\mathbf{x}$ and also

$$\mathcal{F}(m) = \sup_{v \in H^1(\Omega),\ \int_\Omega v d\mathbf{x} = 0} 2\tau \int_\Omega m v d\mathbf{x} - \int_\Omega |\nabla v|^2 d\mathbf{x}.$$

We know that $\int_\Omega v_m d\mathbf{x} = \int_\Omega v_m^* d\mathbf{x}$ due to Brock (2007, Theorem 3.1). Now, employing Lemmas 3 and 4, we observe that

$$\begin{aligned} \mathcal{F}(m) &= \sup_{v \in H^1(\Omega),\ \int_\Omega v d\mathbf{x} = 0} 2\tau \int_\Omega m v d\mathbf{x} - \int_\Omega |\nabla v|^2 d\mathbf{x} \\ &\leq 2\tau \int_\Omega m^* {v_m}^* d\mathbf{x} - \int_\Omega |\nabla {v_m}^*|^2 d\mathbf{x} \\ &\leq \sup_{v \in H^1(\Omega),\ \int_\Omega v d\mathbf{x} = 0} 2\tau \int_\Omega m^* v d\mathbf{x} - \int_\Omega |\nabla v|^2 d\mathbf{x} = \mathcal{F}(m^*), \end{aligned} \tag{13}$$

for an arbitrary direction $\mathbf{e}$. This yields that m^* is a maximizer for (10). □

In the next theorem, we will address the question of uniqueness for (10) when Ω is a ball or an annulus.

Theorem 2 *Let Ω be ball $B(\mathbf{0}, r_2)$ or annulus $B(\mathbf{0}, r_2)\backslash\overline{B(\mathbf{0}, r_1)}$ for some $r_2 > r_1 \geq 0$ in $\mathbb{R}^N$, $N \geq 2$. Then, precisely one of the following statements holds*
a) the problem (10) has a unique and then radial solution,
b) the problem (10) has infinitely many solutions.

Proof a) For an arbitrary direction $\mathbf{e}$, the cap symmetric function χ_{D^*} is a maximizer invoking Theorem 1. Due to the uniqueness, the set D^* is symmetric with respect to all direction since $\mathbf{e}$ is arbitrary. It yields that D^* should be a radial set. b) If there is not a radial solution then indeed we have infinitely many maximizers for (10) in view of Theorem 1. □

4 Numerical method

Our numerical algorithm is based upon the idea of the gradient ascent method. Therefore, in what follows we provide variations of $J(m)$ and $u_{\mu,m}$ with respect to m.

Lemma 8 *Let $m \in \mathcal{M}$, $g \in L^\infty(\Omega)$ and $\epsilon > 0$ such that $m + \epsilon g \in \mathcal{M}$. Then,*
i) there exists $\psi_{\mu,m,g} \in H^1(\Omega)$ such that

$$\frac{u_{\mu,m+\epsilon g} - u_{\mu,m}}{\epsilon} \rightharpoonup \psi_{\mu,m,g} \quad \textit{weakly in} \quad H^1(\Omega),$$

as $\epsilon \longrightarrow 0$ and

$$\begin{cases} \mu\Delta\psi_{\mu,m,g} + (m - 2u_{\mu,m})\psi_{\mu,m,g} = -g u_{\mu,m} & \textit{in} \quad \Omega, \\ \frac{\partial\psi_{\mu,m,g}}{\partial\mathbf{n}} = 0 & \textit{on } \partial\Omega. \end{cases} \tag{14}$$

ii) Moreover, we have

$$\int_\Omega u_{\mu,m+\epsilon g} d\mathbf{x} = \int_\Omega u_{\mu,m} d\mathbf{x} + \epsilon \int_\Omega \psi_{\mu,m,g} d\mathbf{x} + O(\epsilon^2). \tag{15}$$

Proof See Ding et al. (2010, Lemma 4.1) and Nagahara and Yanagida (2018, Proposition 2.2)). □

Rewriting Eq. (15) in the following form

$$\int_\Omega u_{\mu,m+\epsilon g} d\mathbf{x} - \int_\Omega u_{\mu,m} d\mathbf{x} = \epsilon \int_\Omega \psi_{\mu,m,g} d\mathbf{x} + O(\epsilon^2),$$

reveals that for $m \in \mathcal{M}$ and ϵ small enough, Eq. (15) provides an ascend direction to increase $J(m)$ over $\mathcal{M}$ if we have $\int_\Omega \psi_{\mu,m,g} d\mathbf{x} > 0$. The problem is that $\psi_{\mu,m,g}$ depends on the function g and it is not clear that how we can determine g which yields $\psi_{\mu,m,g}$ with positive integral. To overcome this problem, let us consider the following adjoint problem

$$\begin{cases} \mu\Delta w + (m - 2u_{\mu,m})w = -1 & \text{in} \quad \Omega, \\ \frac{\partial w}{\partial\mathbf{n}} = 0 & \text{on } \partial\Omega. \end{cases} \tag{16}$$

This equation has a unique solution $w = w_{\mu,m}$ due to the fact that the operator $\mu\Delta + (m - 2u_{\mu,m})$ is invertible, see Lou (2006) and Nagahara and Yanagida (2018, Proposition 2.2). Using standard elliptic regularity arguments and the Sobolev embedding theorems, we have $w(\mathbf{x}) \in W^{2,p}(\Omega) \cap C^{1,\alpha}(\bar{\Omega})$ for $\alpha \in (0, 1)$ and all $p > 1$. It is noteworthy that there is $C > 0$ such that

$$\|w\|_{L^\infty(\Omega)} \leq C, \tag{17}$$

and C is uniform in $m \in \mathcal{M}$, see Mazari et al. (2020).

Multiplying (14) by w and (16) by $\psi_{\mu,m,g}$ and applying integration by parts, we obtain

$$-\mu \int_\Omega \nabla\psi_{\mu,m,g} \nabla w d\mathbf{x} + \int_\Omega (m - 2u_{\mu,m})\psi_{\mu,m,g} w d\mathbf{x} = -\int_\Omega g u_{\mu,m} w d\mathbf{x},$$
$$-\mu \int_\Omega \nabla w \nabla\psi_{\mu,m,g} d\mathbf{x} + \int_\Omega (m - 2u_{\mu,m}) w \psi_{\mu,m,g} d\mathbf{x} = -\int_\Omega \psi_{\mu,m,g} d\mathbf{x},$$

which reveals that

$$\int_\Omega \psi_{\mu,m,g} d\mathbf{x} = \int_\Omega g u_{\mu,m} w_{\mu,m} d\mathbf{x}. \tag{18}$$

Employing (18), one can determines an ascend direction for $J(m)$ in $\mathcal{M}$ in the following way. Let $\eta \in \mathcal{M}$, $0 < \epsilon < 1$ and assume m is not a local maximizer of $J(m)$ with respect to $\mathcal{M}$. Then $m + \epsilon(\eta - m)$ belongs to $\mathcal{M}$ since $\mathcal{M}$ is convex in view of Lemma 1. Setting $g = \eta - m$ in (18) we have

$$\int_\Omega \psi_{\mu,m,g} d\mathbf{x} = \int_\Omega \eta u_{\mu,m} w_{\mu,m} d\mathbf{x} - \int_\Omega m u_{\mu,m} w_{\mu,m} d\mathbf{x}. \tag{19}$$

Now setting $f(\mathbf{x}) = u_{\mu,m}(\mathbf{x}) w_{\mu,m}(\mathbf{x})$ in Lemma 5, we can compute the maximizer of the first integral on the right-hand side of (19) which is $\eta = \chi_D$ where D is a subset of a super-level set of $f(\mathbf{x}) = u_{\mu,m}(\mathbf{x}) w_{\mu,m}(\mathbf{x})$ derived by (7) and (8). Therefore, starting from m, $g = \chi_D - m$ is a direction for functional $J(m)$ with steepest ascend. One can use a line search algorithm to determine the maximum amount to move along the given ascend direction that the condition $J(m+\epsilon g) > J(m)$ is fulfilled. The resulting algorithm is presented in Algorithm 1.

The following theorem determine the global minimizer of the functional $J(m)$ over $\mathcal{M}$.

Lemma 9 *If $m(\mathbf{x}) = A/|\Omega|$, then for all μ, $u(\mathbf{x}) = m(\mathbf{x})$ is the solution of (1) and $J = A$. Moreover, $m = A/|\Omega|$ is the unique minimizer of $J(m)$ over $\mathcal{M}$.*

Proof A simple calculation yields the first part of theorem. For the proof of the second part see Mazari et al. (2020). □

The following theorem provides an optimality condition for a maximizer of (4) when the diffusion μ is large enough.

Algorithm 1 Maximization algorithm

Given μ, A, and $TOL > 0$, choose an initial $m_0 \in \mathcal{M}$.
1. Set $i = 0$.
2. Compute $u_i = u_{\mu,m_i}$ and $J(u_i)$ using a finite element method.
3. Set $m_i - 2u_i$ as the coefficient in (16) and compute $w_i = w_{\mu,m_i}$ using a finite element method.
4. Set $f = u_i w_i$ and derive χ_{D_i} employing formulas (7) and (8).
5. Set $g_i = \chi_{D_i} - m_i$ and $\epsilon = 1$.
6. Set $m_{i+1} = m_i + \epsilon g_i$ and compute $u_{i+1} = u_{\mu,m_{i+1}}$ and $J(m_{i+1})$ using a finite element method.
7. While $J(m_{i+1}) < J(m_i)$ do
Set $\epsilon = \epsilon/2$.
Set $m_{i+1} = m_i + \epsilon g_i$ and compute u_{i+1} and $J(m_{i+1})$ using a finite element method.
8. If $J(m_{i+1}) - J(m_i) < TOL$, stop the algorithm. Otherwise set $i = i + 1$, go to step 3.

Theorem 3 *Assume diffusion μ is large enough. Then, we have $\hat{m} = \chi_{\hat{D}}$ for $\hat{D} \subset \Omega$ with $|\hat{D}| = A$ such that*

$$\int_\Omega \eta u_{\mu,\hat{m}} w_{\mu,\hat{m}} d\mathbf{x} < \int_\Omega \hat{m} u_{\mu,\hat{m}} w_{\mu,\hat{m}} d\mathbf{x},$$

for all $\eta \in \mathcal{M}$ where $\eta \neq \hat{m}$ and also we have $\hat{D} = \{x \in \Omega : \ u_{\mu,\hat{m}}(\mathbf{x}) w_{\mu,\hat{m}}(\mathbf{x}) \geq \hat{t}\}$.

Proof According to Theorem 1 in Mazari et al. (2020) we know that the maximizer is of bang-bang type and so $\hat{m} = \chi_{\hat{D}}$ for $\hat{D} \subset \Omega$ with $|\hat{D}| = A$ when μ is large enough.

According to (15) and (18) we observe that $J(m)$ is Gateaux differentiable and indeed we have

$$\lim_{\epsilon \to 0^+} \frac{J(m + \epsilon(\eta - m)) - J(m)}{\epsilon} = \int_\Omega (\eta - m) u_{\mu,m} w_{\mu,m} d\mathbf{x}, \tag{20}$$

for all $\eta, m \in \mathcal{M}$.

In view of Theorem 1 in Mazari et al. (2020), $J : \mathcal{M} \to \mathbb{R}$ is strictly convex for large μ and so we see that

$$\frac{J(\hat{m} + \epsilon(\eta - \hat{m})) - J(\hat{m})}{\epsilon} < J(\eta) - J(\hat{m}) \leq 0, \tag{21}$$

for all $\eta \in \mathcal{M}$, $\eta \neq \hat{m}$ and $0 < \epsilon < 1$. On the other hand due to the convexity of $J(m)$ and (20) we have

$$J(\hat{m} + \epsilon(\eta - \hat{m})) \geq J(\hat{m}) + \epsilon \int_\Omega (\eta - \hat{m}) u_{\mu,\hat{m}} \hat{w}_{\mu,\hat{m}} d\mathbf{x},$$

or equivalently

$$\frac{J(\hat{m} + \epsilon(\eta - \hat{m})) - J(\hat{m})}{\epsilon} \geq \int_\Omega (\eta - \hat{m}) u_{\mu,\hat{m}} \hat{w}_{\mu,\hat{m}} d\mathbf{x}, \tag{22}$$

for all $\eta \in \mathcal{M}$ and $0 < \epsilon < 1$. Combining (21) and (22) we have

$$\int_\Omega \eta u_{\mu,\hat{m}} \hat{w}_{\mu,\hat{m}} d\mathbf{x} < \int_\Omega \hat{m} u_{\mu,\hat{m}} \hat{w}_{\mu,\hat{m}} d\mathbf{x}, \tag{23}$$

for all $\eta \in \mathcal{M}$ where $\eta \neq \hat{m}$. This means that $\hat{m}$ is the unique maximizer of the functional $L(\eta) = \int_\Omega \eta u_{\mu,\hat{m}} \hat{w}_{\mu,\hat{m}} d\mathbf{x}$ over $\mathcal{M}$. Employing Theorem 4.5 in Burton (1987) there is an increasing function $\xi : \mathbb{R} \to \mathbb{R}$ such that $\hat{m} = \chi_{\hat{D}} = \xi(u_{\mu,\hat{m}} \hat{w})$. This yields the last assertion of the theorem. □

In the next theorem we will address the convergence of Algorithm 1. Recall that the algorithm generates an increasing sequence of $\{J(m_i)\}_1^\infty$ which is bounded from above and so it converges to its supremum denoted by $\hat{J}$. We establish that every accumulation point of the sequence $\{m_i\}_1^\infty$ generated by the algorithm is a stationary point and indeed satisfies the necessary condition for the maximizer. Let us recall that $\hat{m} \in \mathcal{M}$ is an accumulation point of the sequence generated by Algorithm 1 if there exists a subsequence, still denoted by $\{m_i\}_1^\infty$, such that $m_i \rightharpoonup \hat{m}$ weakly in $L^2(\Omega)$.

Theorem 4 *i) For all accumulation point $\hat{m} \in \mathcal{M}$ such that $m_i \rightharpoonup \hat{m}$ weakly in $L^2(\Omega)$ we have $u_i \to \hat{u} = u_{\mu,\hat{m}}$ strongly in $L^2(\Omega)$ and $J(m_i) \to \hat{J} = J(\hat{m})$.*
ii) Let $\hat{w} = w_{\mu,\hat{m}}$. We have

$$\int_\Omega \hat{m}\hat{u}\hat{w} d\mathbf{x} \geq \int_\Omega \eta\hat{u}\hat{w} d\mathbf{x}, \quad \textit{for all } \ \eta \in \mathcal{M}. \tag{24}$$

iii) Assume all level sets of function $\hat{u}(\mathbf{x})\hat{w}(\mathbf{x})$ have zero Lebesgue measure. Then, we have $\hat{m} = \chi_{\hat{D}}$ where $\hat{D} = \{x \in \Omega : \hat{u}(\mathbf{x})\hat{w}(\mathbf{x}) \geq \hat{t}\}$ with $|\hat{D}| = A$ and $m_i \to \hat{m}$ strongly in $L^2(\Omega)$.

Proof i) In view of Eq. (1), we obtain

$$\mu \int_\Omega |\nabla u_i|^2 d\mathbf{x} = \int_\Omega m_i u_i^2 d\mathbf{x} - \int_\Omega u_i^3 d\mathbf{x} \leq \int_\Omega m_i u_i^2 d\mathbf{x} \leq |\Omega|,$$

due to (2). Therefore, we can conclude that $\|u_i\|_{H^1(\Omega)}$ is bounded and so there is $\hat{u} \in H^1(\Omega)$ and a subsequence, still denoted by $\{u_i\}_1^\infty$, such that $u_i \rightharpoonup \hat{u}$ in $H^1(\Omega)$. Sobolev embedding yields that $u_i \to \hat{u}$ in $L^2(\Omega)$. In summary, we have

$$m_i \rightharpoonup \hat{m}, \ u_i \to \hat{u} \quad \text{in } L^2(\Omega) \quad \text{and} \quad u_i \rightharpoonup \hat{u} \quad \text{in } H^1(\Omega). \tag{25}$$

In view of (2) and (25), it is inferred that $\|\hat{u}\|_{L^\infty(\Omega)} \leq 1$.

It just remains to prove that $\hat{u} = u_{\mu,\hat{m}}$. The weak form of (1) gives

$$-\int_\Omega \nabla u_i \cdot \nabla \phi d\mathbf{x} + \int_\Omega m_i u_i \phi d\mathbf{x} - \int_\Omega u_i^2 \phi d\mathbf{x} = 0, \quad \text{for all} \quad \phi \in H^1(\Omega). \tag{26}$$

Now, it is observed that when $i \to \infty$

$$\left|\int_\Omega (m_i u_i \phi - \hat{m}\hat{u}\phi) d\mathbf{x}\right| \le \left|\int_\Omega m_i(u_i\phi - \hat{u}\phi) d\mathbf{x}\right| + \left|\int_\Omega (m_i - \hat{m})\hat{u}\phi d\mathbf{x}\right| \to 0,$$

due to the facts that $\|m_i\|_{L^\infty(\Omega)} \le 1$, $\|\hat{u}\|_{L^\infty(\Omega)} \le 1$ and (25). Furthermore, we have

$$\left|\int_\Omega u_i^2\phi - \hat{u}^2\phi d\mathbf{x}\right| \le \left|\int_\Omega (u_i + \hat{u})(u_i - \hat{u})\phi d\mathbf{x}\right| \le 2\|u_i - \hat{u}\|_{L^2(\Omega)}\|\phi\|_{L^2(\Omega)} \to 0,$$

in view of boundedness of u_i and $\hat{u}$ and (25). Consequently, passing to the limit in (26), we obtain $\hat{u} = u_{\mu,\hat{m}}$. It is straightforward that $J(m_i) \to J(\hat{m})$. Recall that $\{J(m_i)\}_1^\infty$ is a subsequence of a convergent sequence and hence we have $\hat{J} = J(\hat{m})$.
ii) Recall that according to Algorithm 1, $J(m_i) < J(m_{i+1})$ and so

$$J(\hat{m}) = \sup\{J(m_i) : i \in \mathbb{N}\}. \tag{27}$$

This yields that

$$\int_\Omega \hat{m}\hat{u}\hat{w} d\mathbf{x} \ge \int_\Omega \eta\hat{u}\hat{w} d\mathbf{x}, \quad \text{for all } \eta \in \mathcal{M}, \tag{28}$$

since otherwise, as explained above, we can find $\bar{m} \in \mathcal{M}$ such that $J(\bar{m}) > J(\hat{m})$. This contradicts (27).
iii) Equation (28) says that $\hat{m}$ is a maximizer of the functional $L(\eta) = \int_\Omega \eta\hat{u}\hat{w} d\mathbf{x}$ for $\eta \in \mathcal{M}$. Since every level set of $\hat{u}\hat{w}$ has zero measure, there is an increasing function $\xi : \mathbb{R} \to \mathbb{R}$ such that $\xi(\hat{u}\hat{w}) \in \mathcal{N}$, see Burton (1989, Lemma 2.9). The function $\xi(\hat{u}\hat{w})$ is the unique maximizer of $L(\eta)$ relative to $\mathcal{M}$ in view of Burton (1989, Lemma 2.4). Hence, one can infer that $\hat{m} = \xi(\hat{u}\hat{w}) = \chi_{\hat{D}}$ and so we should have

$$\xi(s) = \begin{cases} 0 & s < \hat{t}, \\ 1 & s \ge \hat{t}, \end{cases}$$

and $\hat{D} = \{x \in \Omega : \hat{u}(\mathbf{x})\hat{w}(\mathbf{x}) \ge \hat{t}\}$ such that $|\hat{D}| = A$. In order to show the strong convergence of the sequence $\{m_i\}_1^\infty$, we see that

$$\begin{aligned} \|m_i - \hat{m}\|^2_{L^2(\Omega)} &= \|m_i\|^2_{L^2(\Omega)} + \|\hat{m}\|^2_{L^2(\Omega)} - 2\int_\Omega m_i\hat{m} d\mathbf{x} \\ &\le 2\|\hat{m}\|^2_{L^2(\Omega)} - 2\int_\Omega m_i\hat{m} d\mathbf{x}, \end{aligned} \tag{29}$$

in view of Lemma 2. Passing $i \to \infty$ in (29), we obtain the strong convergence result. □

Remark 1 It is noteworthy that while μ is large enough we can always consider $\epsilon = 1$ in Algorithm 1 and it is not required to use procedures like the line search algorithm to determine the maximum amount to move along the given ascend direction. It is due to the fact that functional J is strictly convex for such μ and then we have

$$J(m_{i+1}) = J(m_i + \epsilon g_i) > J(m_i) + \epsilon \int_\Omega g_i u_i w_i d\mathbf{x}.$$

4.1 Numerical Implementations

In this section, we show numerical results of Algorithm 1 to determine the optimal $\hat{m}(\mathbf{x})$ which maximizes J, the total population of species. For any given diffusion constant μ and area constant A such that $m(\mathbf{x}) \in \mathcal{M}$, we use numerical approaches to find the solution $u(\mathbf{x})$ to Eq. (1). In one dimension, a collocation method is used and implemented by MATLAB built-in function bvp4c. The initial mesh has 12001 grid points. In two dimensions, a finite element method is used and the basis functions are linear polynomials of degree one. The resulting discretized nonlinear system is solved by Gauss-Newton iteration method with numerical evaluation of the full Jacobian. The residual tolerance to terminate the nonlinear solver is 10^{-10}. The tolerance to stop Algorithm 1 is chosen as 10^{-6}. The implementation is done in MATLAB by using a PDE Toolbox. For optimization problem, we start with many different random resource functions m and report the optimizer which achieves the maximal total population size J.

To emphasize the dependence of the total population on the resource function $m(\mathbf{x})$ and the diffusion constant, we will use the notation $J = J(m(\mathbf{x}), \mu)$ from now on. In Fig. 1, we show how the total population size J changes with respect to the diffusion constant μ for the resource function $m(x) = m_1(x) := \chi_{[0.7,1]}$ and $m(x) = m_2(x) := \chi_{[0.35,0.65]}$. As discussed in Lou (2006), the total population size reaches minimums, $J = \int m_1(x)dx = 0.3$, at $\mu = 0$ and $\mu = \infty$, and a maximum at some intermediate $\mu^\star$. In this case, $J(m_1, \mu^\star) \approx 0.406$ at $\mu^\star \approx 0.035279$. Note that due to the symmetry, $J(\chi_{[0,0.3]}, \mu) = J(\chi_{[0.7,1]}, \mu)$. In Fig. 1b, the resource function is chosen as $\chi_{[0.35,0.65]}$, the graph of the total population size J is similar to the one in Fig. 1 and the total population size reaches a maximum $J(m_2, \mu^\star) \approx 0.406$ at $\mu^\star \approx 0.008819$. Indeed, the values of total population satisfies $J(m_1(x), \mu) = J(m_2(x), \frac{\mu}{4})$. When the logarithmic scale is used for the x-axis, the graph of J for $m_2(x)$ shifts to the left by $\log_{10} 4$ comparing to the one for $m_1(x)$.

In Fig. 2, we show the total population for $m(x) = \chi_{[c-0.15,c+0.15]}$ for $c \in [0.5, 0.85]$. Among this class of resource functions, the optimal resource function is $\hat{m}(x) = m_1(x)$ when μ is greater than 0.01589 while the optimal resource $\hat{m}(x) = m_2(x)$ when μ is smaller than 0.01589.

In Fig. 3, we show how J varies with respect to the diffusion constant μ for another two resource functions $m(x) = \chi_{[0.05,0.1]} + \chi_{[0.15,0.35]} + \chi_{[0.5,0.55]} + \chi_{[0.85,0.9]}$ and $m(x) = \chi_{[0,0.05]} + \chi_{[0.1,0.25]} + \chi_{[0.45,0.5]} + \chi_{[0.85,0.9]}$, respectively. As indicated in Liang and Lou (2012), the total population size is usually not a monotone function of the diffusion constant μ. In Fig. 3a, the total population size has two local maxima and one local minimum.

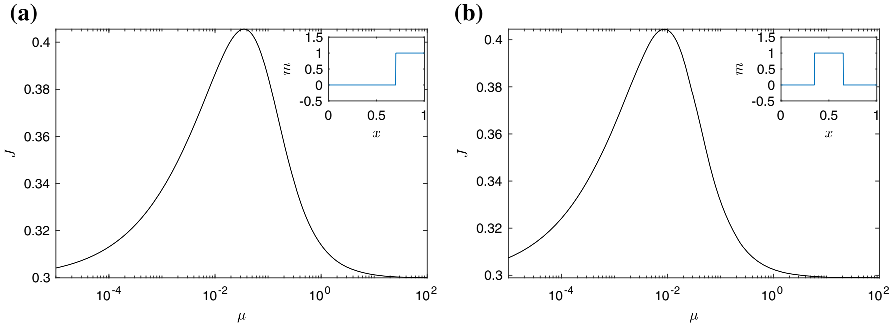

Fig. 1 The graph of the total population $J(m(x), \mu)$ with respect to μ for the resource function **a** $m(x) = m_1(x) := \chi_{[0.7,1]}$ and **b** $m(x) = m_2(x) := \chi_{[0.35,0.65]}$

In general, assume that $u(x)$ is the solution of (1.1) with $m(x) = \chi_{[1-l,1]}$ on [0, 1] with a given constant $l > 0$. For a given positive integer k, denote $x_j = \frac{j}{k}, 0 \le j \le k-1$,

$$m_k(x) = \begin{cases} m\left(k\left(x - x_j\right)\right) & x_j \le x \le x_{j+1},\ j = \text{even}, \\ m\left(k\left(x_{j+1} - x\right)\right) & x_j \le x \le x_{j+1},\ j = \text{odd}, \end{cases}$$

and

$$u_k(x) = \begin{cases} u\left(k\left(x - x_j\right)\right) & x_j \le x \le x_{j+1},\ j = \text{even}, \\ u\left(k\left(x_{j+1} - x\right)\right) & x_j \le x \le x_{j+1},\ j = \text{odd}. \end{cases}$$

It is straight forward to verify that

$$\begin{cases} \frac{\mu}{k^2}\Delta u_k + u_k(m_k - u_k) = 0 & x \in \Omega, \\ \frac{\partial u_k}{\partial \mathbf{n}} = 0 & x \in \partial\Omega. \end{cases}$$

where $\Omega = [0, 1]$. In Fig. 4, we see that objective function J remains constant for $\mu = \mu_0/k^2$ and m_k for $\mu_0 = 0.035279$, $m(x) = \chi_{[0.7,1]}$ and $k = 1, 2, 3, 4, 5$ and 6. In light of this, we can use the maximum of the total population with respect to a given class of resource functions such as $m_k(x)$, $k = 1, 2, \cdots$, to provide a lower bound for $J^\star = \max_{m(x)} J(m(x), \mu)$. In Fig. 5, the black curve shows the lower bound for $J^\star$. This indicates that it is possible to find $J^\star \ge 0.406$ for small μ even though it is challenging to obtain this numerically as it requires very refined calculations to achieve the accuracy.

In Figs. 6 and 7, we show the optimal resource functions $\hat{m}(x)$ and its corresponding $\hat{u}(x)$ for the total resource $A = |D|$ equals to 0.3 and 0.6, respectively. In all cases, the optimal resource functions are periodic. Denote $m_1 = \chi_{[0.7,1]}$. The optimal resource functions are $m_1, m_2, m_3, m_6, m_8, m_{19}$ for $\mu = 0.1, 0.01, 0.005, 0.001, 0.0005, 0.0001$, respectively. When μ gets smaller, the optimal resource becomes more fragmented. We also marked these diffusion parameters in red dots in Fig. 5 for $A = 0.3$. Numerically,

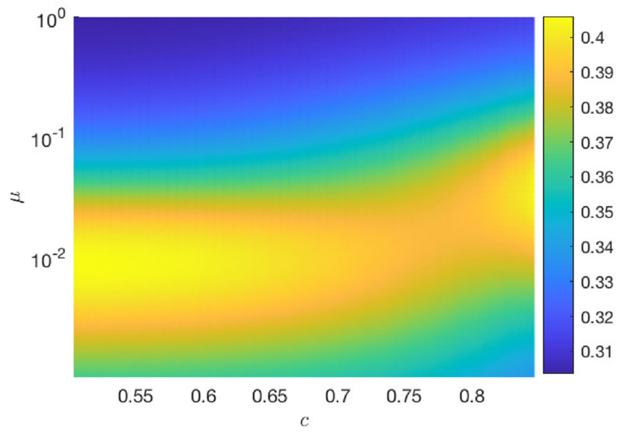

Fig. 2 The resource function $m(x) = \chi_{[c-0.15,c+0.15]}$ for $c \in [0.5, 0.85]$ and its corresponding J with respect to μ

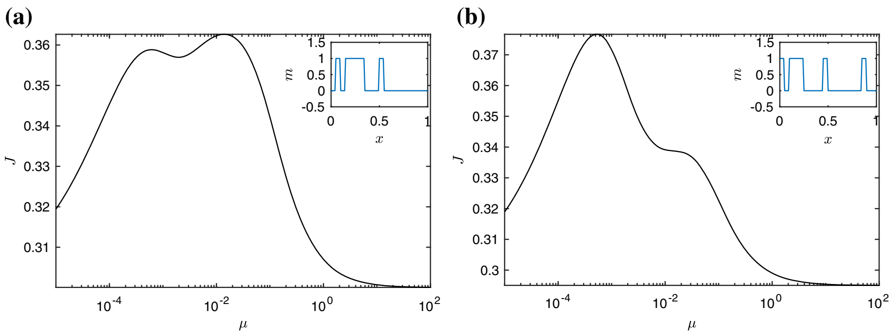

Fig. 3 The graph of the total population $J(m(x), \mu)$ with respect to μ for the resource function **a** $m(x) = \chi_{[0.05,0.1]} + \chi_{[0.15,0.35]} + \chi_{[0.5,0.55]} + \chi_{[0.85,0.9]}$ and **b** $m(x) = \chi_{[0,0.05]} + \chi_{[0.1,0.25]} + \chi_{[0.45,0.5]} + \chi_{[0.85,0.9]}$

we observe some nonperiodic resource functions could be local maximizers as the ones reported in Mazari and Ruiz-Balet (2021). In particular, there are many local maximizers when μ is small. This leads to a big challenge to find the global maximizer for a small diffusion rate.

In two dimensions, we first show results on the unit square $\Omega = [0, 1]^2$. We compute the optimal resource function m for the same parameters that was used in Mazari and Ruiz-Balet (2021). The triangular mesh has 90,876 elements. In Fig. 8, we show the optimal $\hat{m}(\mathbf{x}) = \chi_{\hat{D}}$ and its corresponding $\hat{u}(\mathbf{x})$ for $A = 0.3|\Omega|$ and $\mu = 0.1, 0.01, 0.005$, and 0.001, respectively. For large enough μ, such as $\mu = 0.1$, the optimal domain $\hat{D}$ is simply-connected and attach to one of 4 corners of the square. This result is in line with a theoretical conclusion of Mazari et al. (2020, Theorem 2) which asserts that concentration occurs for large μ.

It is clear that the optimal $\hat{m}(\mathbf{x})$ is not unique. When μ gets smaller, the optimal domain $\hat{D}$ gets more fragmented. Also, the optimal domain $\hat{D}$ and Ω do not possess

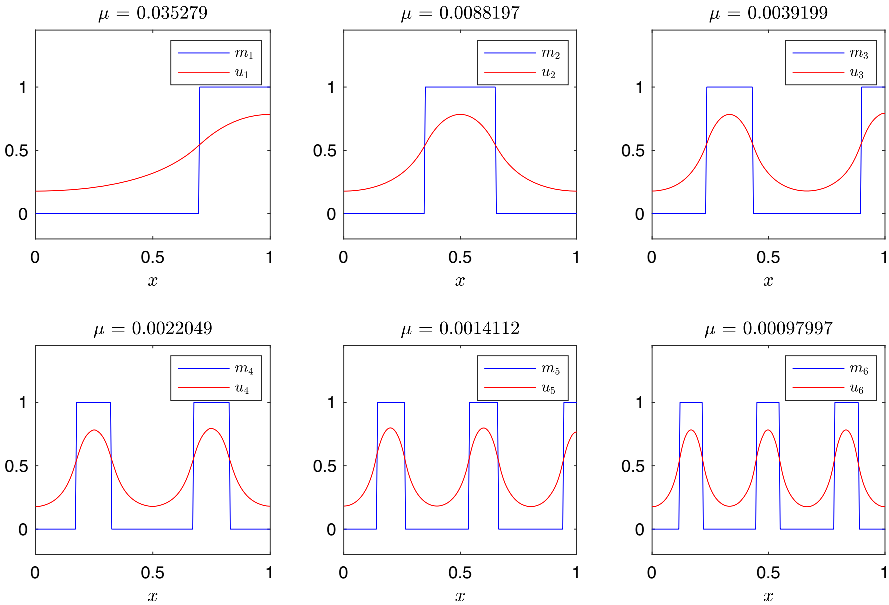

Fig. 4 The solution $u_k(x)$ shown in red for $m(x) = m_k(x)$ shown in blue with $m_1(x) = \chi_{[0.7,1]}$ and $\mu = 0.035279/k^2$ for $k = 1, 2, 3, 4, 5, 6$. All six resource functions leads to the same total population $J \approx 0.406$

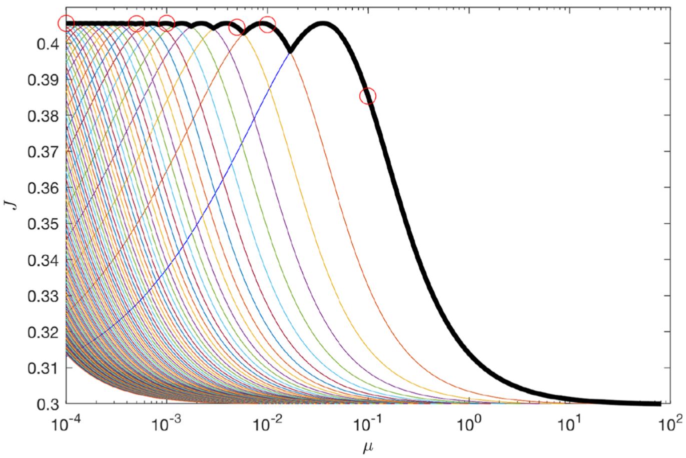

Fig. 5 The lower bound for $J^\star$ is shown in the black curve which is generated by taking the maximum of $J(m_k(x), \mu)$ with $m_1(x) = \chi_{[0.7,1]}$ and $k \in \mathbb{N}$

the same symmetry in general. The maximizers that we found for small μ are different from the ones reported in Mazari and Ruiz-Balet (2021). We have also shown other local maximizers that we found in Fig. 9 and these two configurations are similar to the ones in Mazari and Ruiz-Balet (2021). It is noteworthy to mention that the ones in Fig. 8 have slightly higher total population size even though we only show J with

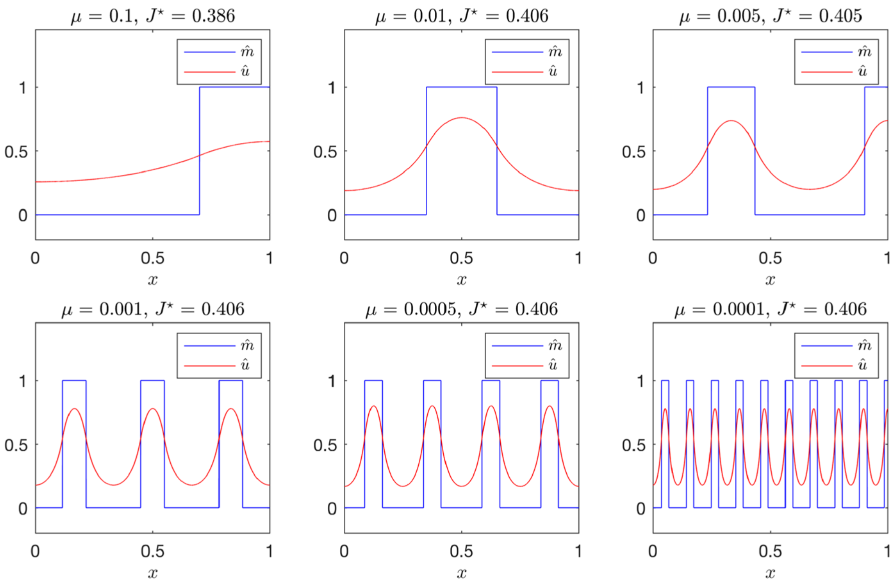

Fig. 6 The optimal resource functions $\hat{m}(x)$ and its corresponding $\hat{u}(x)$ for $A = 0.3$ and different diffusion constants

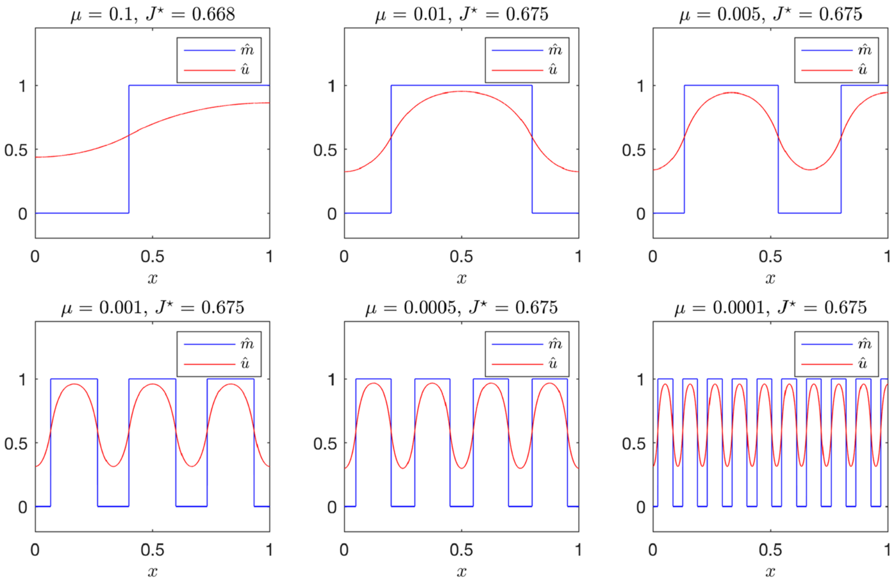

Fig. 7 The optimal resource functions $\hat{m}(x)$ and its corresponding $\hat{u}(x)$ for $A = 0.6$ and different diffusion constants

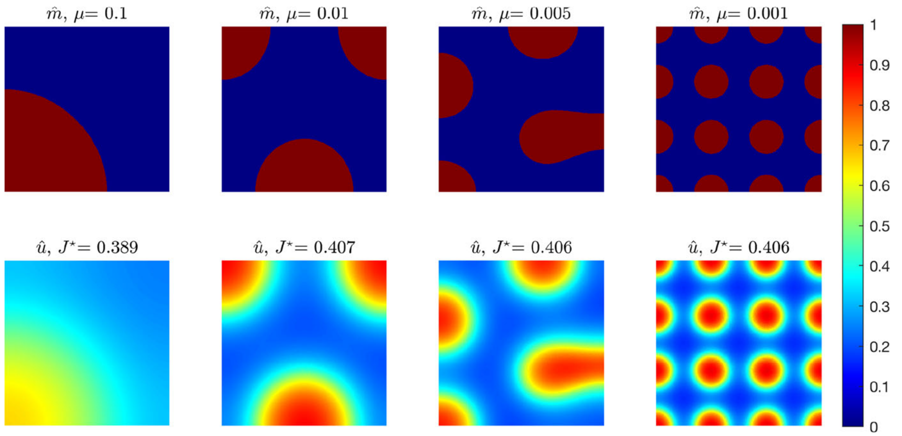

Fig. 8 The optimal $\hat{m}(\mathbf{x})$ and its corresponding $\hat{u}(\mathbf{x})$ for $A = 0.3|\Omega|$ and different diffusion constant μ

three digits after the decimal place. We found that it is quite crucial to choose small enough residual tolerance for the nonlinear solver and use a refined mesh to ensure the accuracy of J.

In Fig. 10, we show the results for $A = 0.6|\Omega|$. When $\mu = 0.1$, the domain $\hat{D}$ is a stripe which is leaning to the side of the square. Again, the optimal $\hat{m}(\mathbf{x})$ is not unique. For $\mu = 0.01$, the domain $\hat{D}$ is a stripe in the center of the square. When $\mu = 0.005$, the domain $\hat{D}$ is no longer simply-connected. The maximizers $\hat{m}(\mathbf{x})$ for $\mu = 0.01$ and $\mu = 0.005$ are different from the ones reported in Mazari and Ruiz-Balet (2021) and have larger total population sizes.

Figures 11 and 12 show results on a L-shaped domain for $A = 0.3|\Omega| = 0.225$ and $A = 0.6|\Omega| = 0.45$, respectively. The triangular mesh has 68,830 elements. Again, the maximizers for large μ, such as $\mu = 0.1$, has a simply-connected domain $\hat{D}$ while the ones for small μ has $\hat{D}$ fragmented. Even when the diffusion constant is small, the optimal $J^\star$ is well beyond the total resource $A = |\hat{D}|$.

Figures 13 and 14 show results on a unit disk for $A = 0.3|\Omega|$ and $A = 0.6|\Omega|$, respectively. The triangular mesh has 116,466 elements. As proved in Theorems 1–2, when μ is large, we expect that the optimal $\hat{m}(\mathbf{x})$ has either a radial or cap symmetry. We observe this phenomenon numerically. For $\mu = 0.1$, the optimal $\hat{m}(\mathbf{x})$ has a cap symmetry and thus one expect that there are infinite solutions due to rotation invariance. When $\mu = 0.05$, the maximizer looks like a projected baseball configuration. When μ is even smaller, we observe that the optimal $\hat{D}$ has several connected components for $A = 0.3|\Omega|$ in Fig. 13 while the complement of the optimal $\hat{D}$ has several connected components for $A = 0.6|\Omega|$ in Fig. 14.

Figures 15 and 16 show results for $A = 0.3|\Omega|$ and $A = 0.6|\Omega|$, respectively, on an annulus with inner radius 0.5 and the outer radius 1. The triangular mesh has 87,766 elements. For $\mu = 0.1$, the optimal resource $\hat{m}(\mathbf{x})$ has a cap symmetry as expected from Theorem 1. In Fig. 15, the optimal $\hat{D}$ becomes more fragmented, having $1, 2, 6, 7$ connected components when $\mu = 0.1, 0.05, 0.01, 0.005$, respectively. For $A = 0.6|\Omega|$, we found a radial maximizer for $\mu = 0.01$ as shown in Fig. 16.

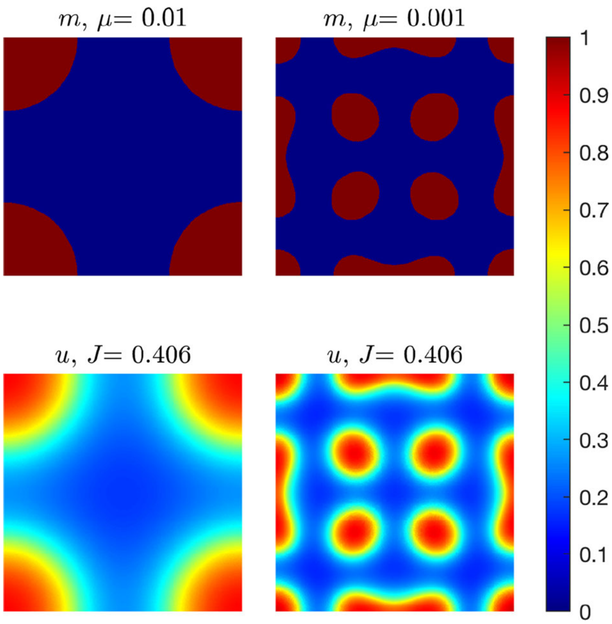

Fig. 9 The other local maximizer $m(\mathbf{x})$ and its corresponding $u(\mathbf{x})$ for $A = 0.3|\Omega|$ and different diffusion constant $\mu = 0.01$ and $\mu = 0.001$, respectively

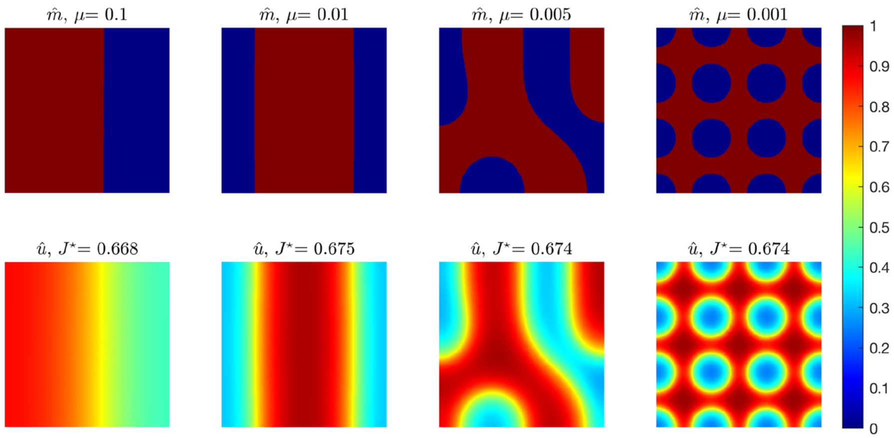

Fig. 10 The optimal $\hat{m}(\mathbf{x})$ and its corresponding $\hat{u}(\mathbf{x})$ for $A = 0.6|\Omega|$ and different diffusion constant μ

5 Conclusion

In this paper we have obtained symmetric properties of the maximizer $\hat{m}$ when Ω is a ball or annulus in $\mathbb{R}^N$ and μ is large. These qualitative properties are in line with results in Mazari et al. (2020) and Mazari and Ruiz-Balet (2021) which assert that for large diffusion, concentrated resources is favourable for maximizing the total population. After deriving an optimality condition, a numerical algorithm has been developed

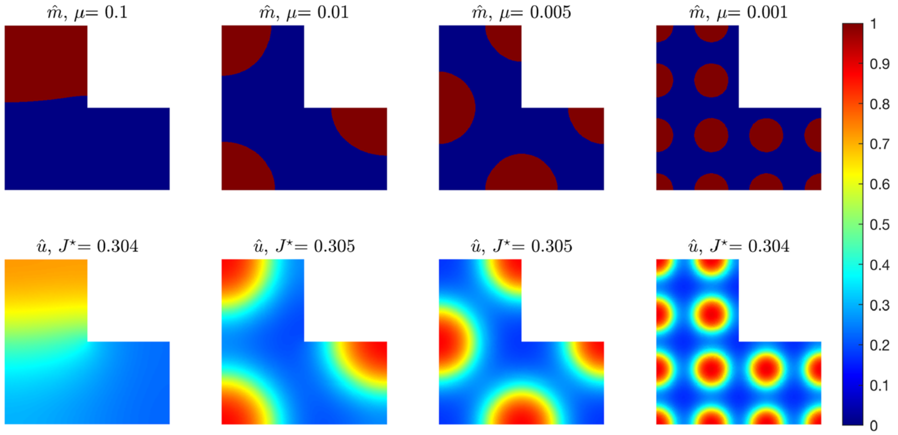

Fig. 11 The optimal $\hat{m}(\mathbf{x})$ and its corresponding $\hat{u}(\mathbf{x})$ for $A = 0.3|\Omega|$ and different diffusion constant μ

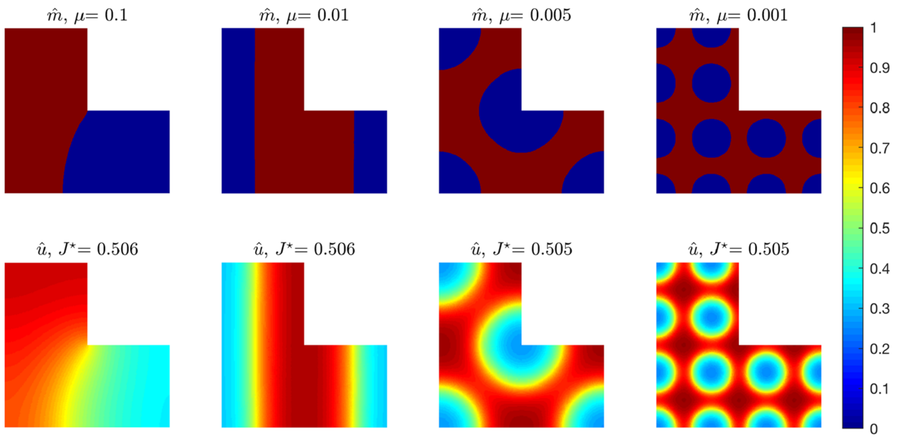

Fig. 12 The optimal $\hat{m}(\mathbf{x})$ and its corresponding $\hat{u}(\mathbf{x})$ for $A = 0.6|\Omega|$ and different diffusion constant μ

based upon rearrangement techniques. It has been proved that the algorithm converges and numerical illustrations reveal that the algorithm can be applied efficiently for domains with different geometries. Our numerical results validate the the theoretical achievement in Ding et al. (2010), Mazari et al. (2020, 2021), and Nagahara and Yanagida (2018), that there is a bang-bang type maximizer for (4) regardless of the value of $\mu > 0$.

To investigate the questions raised in Ding et al. (2010), Mazari and Ruiz-Balet (2021), our numerical results reveal that it is not true that for general domains the optimal resources distribution touches the boundary, see for instance Fig. 6. However, in two dimensions, we observe that the optimal resources distribution touches the boundary for all μ. Moreover, when μ is small and the domain Ω is curved, it is not necessary to allocate the resource only near the curved parts. The resource could also be allocated far away from the curved boundary as shown in Fig. 13. According

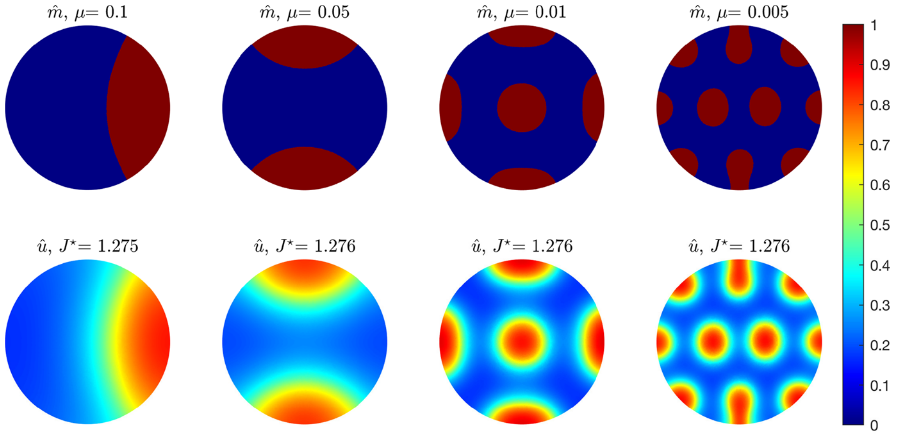

Fig. 13 The optimal $\hat{m}(\mathbf{x})$ and its corresponding $\hat{u}(\mathbf{x})$ for $A = 0.3|\Omega|$ and different diffusion constant μ

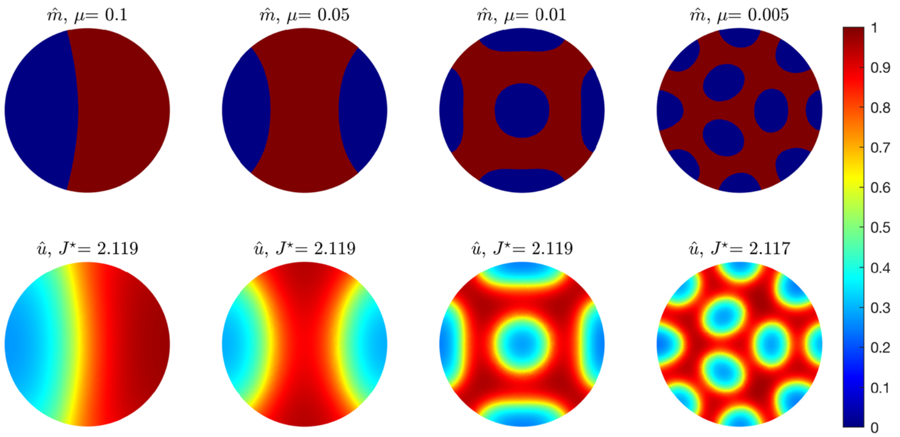

Fig. 14 The optimal $\hat{m}(\mathbf{x})$ and its corresponding $\hat{u}(\mathbf{x})$ for $A = 0.6|\Omega|$ and different diffusion constant μ

to our numerical results in two-dimensional problems, we conjecture that for large enough μ the optimal resources distribution is a simply connected domain touching the boundary. If one can prove that there is a maximum point on the boundary of domain Ω for $u_{\mu,\hat{m}}w_{\mu,\hat{m}}$, then in view of the optimality condition we can conclude that there is a connected component of the optimal resources distribution touching the boundary. Even this simpler assertion is a challenging question.

A highly challenging problem is to investigate the behavior of maximizers as $\mu \to 0$ even for $\Omega = (0, 1)$. The numerical results for one-dimensional problems again validate the theoretical results that to maximize the total population size, the smaller the diffusivity, the more fragmentation should be done. This problem was raised in Mazari et al. (2020). Recently, it has been proved that resource fragmentation is better than concentration for the n-dimensional box domain (Mazari and Ruiz-Balet 2021)

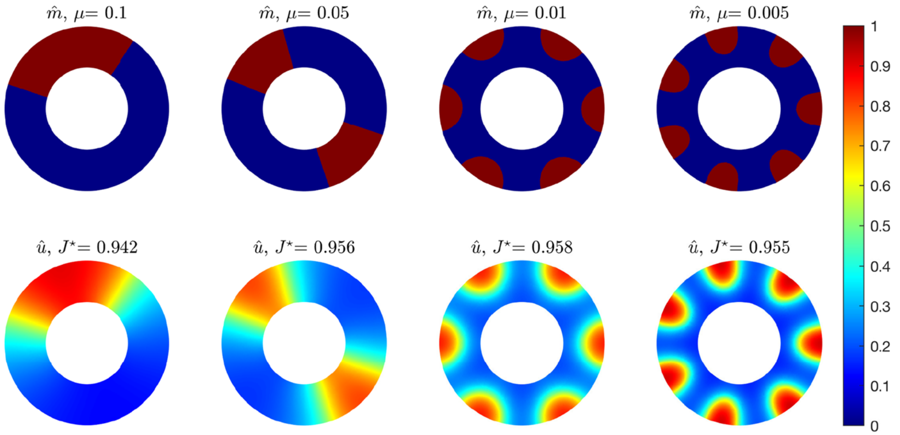

Fig. 15 The optimal $\hat{m}(\mathbf{x})$ and its corresponding $\hat{u}(\mathbf{x})$ for $A = 0.3|\Omega|$ and different diffusion constant μ

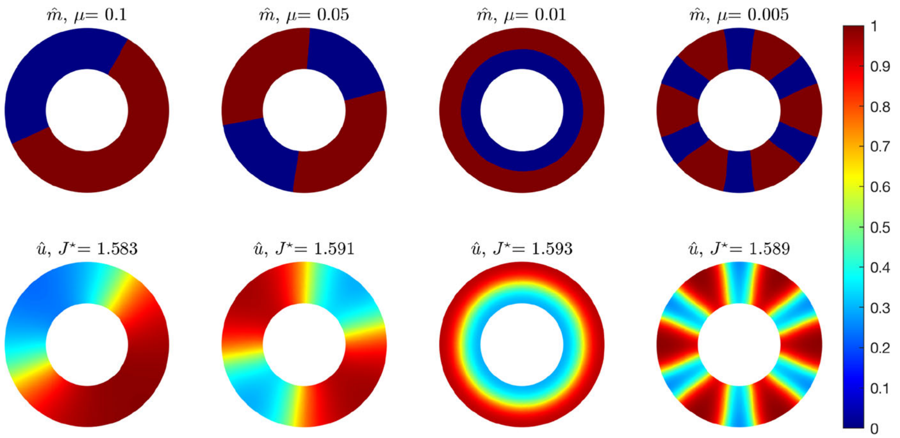

Fig. 16 The optimal $\hat{m}(\mathbf{x})$ and its corresponding $\hat{u}(\mathbf{x})$ for $A = 0.6|\Omega|$ and different diffusion constant μ

and then for any general bounded domains in $\mathbb{R}^N$ if the diffusion rate is sufficiently small (Heo and Kim 2021).

Our numerical investigations illustrate that in the one-dimensional case while $\mu \to 0$ we can find maximizers with periodic pattern, see Figs. 4, 6 and 7. However, it is hard to conclude the same pattern for two-dimensional problems. Moreover, in this case, the numerical results of this paper suggest that when $\mu \to 0$ the total variation of $\hat{m}_\mu$ goes to infinity as it has been proved in Theorem 1 of Mazari and Ruiz-Balet (2021).

Based upon our two-dimensional illustrations, we cannot infer decisively about the topology and geometry of the optimal domain $\hat{D}$ for small diffusivity although it has been proved that fragmentation phenomenon occurs (Mazari and Ruiz-Balet 2021; Heo and Kim 2021). According to Figs. 8, 11, 13 and 15, while A or the total amount of resources is small, fragmentation occurs which means that the total variation of the function $\hat{m}_\mu$ goes to infinity while $\mu \to 0$. However, the set $\hat{D}$ is disconnected and has a lot of connected components. But, if A is large, the optimal resource distribution is fragmented and in this case it is connected, see for instance Figs. 10, 12 and 14. Indeed, it seems that for the case that A is large, the set $\hat{D}^c$ corresponding to the maximizer $\hat{m} = \chi_{\hat{D}}$ or the places which is not favourable to the species, is disconnected and has many connected components while we can observe that the total variation of the function $\hat{m}_\mu$ goes to infinity as $\mu \to 0$. These observation necessitate a study on the topology and geometry of the optimal domain $\hat{D}$ considering both factors A, the total amount of resources, and μ, the diffusivity.

Author Contributions The authors contributed equally to this work.

Funding Chiu-Yen Kao's work is supported in part by NSF grants DMS-1818948 and DMS-2208373.

Data Availability Numerical results generated during the current study are available in the Zenodo repository, https://doi.org/10.5281/zenodo.5525494 (Kao and Mohammadi 2020).

Code Availability The codes are avaliable in the Zenodo repository, https://doi.org/10.5281/zenodo.5525494 (Kao and Mohammadi 2020).

Declarations

Conflict of interest Not applicable.

References

Bai X, He X, Li F (2016) An optimization problem and its application in population dynamics. Proc Am Math Soc 144(5):2161–2170. https://doi.org/10.1090/proc/12873

Berestycki H, Hamel F, Roques L (2005) Analysis of the periodically fragmented environment model: I—species persistence. J Math Biol 51(1):75–113. https://doi.org/10.1007/s00285-004-0313-3

Brock F (2007) Chapter 1—rearrangements and applications to symmetry problems in PDE. In: Chipot M (ed) Stationary partial differential equations. Handbook of differential equations: stationary partial differential equations, vol 4. North-Holland, Amsterdam, pp 1–60. https://doi.org/10.1016/S1874-5733(07)80004-0

Burton G (1987) Rearrangements of functions, maximization of convex functionals, and vortex rings. Math Ann 276(2):225–253. https://doi.org/10.1007/BF01450739

Burton G (1989) Variational problems on classes of rearrangements and multiple configurations for steady vortices. Annales de l'Institut Henri Poincare (C) Non Linear Anal 6:295–319

Cantrell RS, Cosner C (1989) Diffusive logistic equations with indefinite weights: population models in disrupted environments. Proc R Soc Edinb Sect A: Math 112(3–4):293–318. https://doi.org/10.1017/S030821050001876X

Cantrell RS, Cosner C (1991) The effects of spatial heterogeneity in population dynamics. J Math Biol 29(4):315–338. https://doi.org/10.1007/BF00167155

Chugunova M, Jadamba B, Kao C-Y, Klymko C, Thomas E, Zhao B (2016). Study of a mixed dispersal population dynamics model. In: Topics in numerical partial differential equations and scientific computing. Springer, New York, NY, pp 51–77. https://doi.org/10.1007/978-1-4939-6399-7_3

Cosner C, Cuccu F, Porru G (2013) Optimization of the first eigenvalue of equations with indefinite weights. Adv Nonlinear Stud 13(1):79–95. https://doi.org/10.1515/ans-2013-0105

Ding W, Finotti H, Lenhart S, Lou Y, Ye Q (2010) Optimal control of growth coefficient on a steady-state population model. Nonlinear Anal Real World Appl 11(2):688–704. https://doi.org/10.1016/j.nonrwa.2009.01.015

Gilbarg D, Trudinger NS (2015) Elliptic partial differential equations of second order. Springer, Berlin

Goss-Custard J, Stillman R, Caldow R, West A, Guillemain M (2003) Carrying capacity in overwintering birds: when are spatial models needed? J Appl Ecol 40(1):176–187. https://doi.org/10.1046/j.1365-2664.2003.00785.x

Hardy GH, Littlewood JE, Pólya G, Pólya G et al (1952) Inequalities. Cambridge University Press, Cambridge

He X, Ni W-M (2016a) Global dynamics of the Lotka–Volterra competition–diffusion system: diffusion and spatial heterogeneity I. Commun Pure Appl Math 69(5):981–1014

He X, Ni W-M (2016b) Global dynamics of the Lotka–Volterra competition–diffusion system with equal amount of total resources, II. Calc Var Partial Differ Equ 55(2):25

He X, Ni W-M (2017) Global dynamics of the Lotka–Volterra competition–diffusion system with equal amount of total resources, III. Calc Var Partial Differ Equ 56(5):132. https://doi.org/10.1007/s00526-017-1234-5

Heo J, Kim Y (2021) On the fragmentation phenomenon in the population optimization problem. Proc Am Math Soc 149(12):5211–5221

Hintermüller M, Kao C-Y, Laurain A (2012) Principal eigenvalue minimization for an elliptic problem with indefinite weight and robin boundary conditions. Appl Math Optim 65(1):111–146. https://doi.org/10.1007/S00245-011-9153-X

Kao C-Y, Mohammadi SA (2020) Maximal total population of species in a diffusive logistic model. https://doi.org/10.5281/zenodo.5525494

Kao C-Y, Lou Y, Yanagida E (2008) Principal eigenvalue for an elliptic problem with indefinite weight on cylindrical domains. Math Biosci Eng 5(2):315. https://doi.org/10.3934/mbe.2008.5.315

Kawohl B (2006) Rearrangements and convexity of level sets in PDE, vol 1150. Springer, Berlin

Lam K-Y, Liu S, Lou Y (2020) Selected topics on reaction–diffusion–advection models from spatial ecology. arXiv preprint arXiv:2004.07978. https://doi.org/10.5206/mase/10644

Lamboley J, Laurain A, Nadin G, Privat Y (2016) Properties of optimizers of the principal eigenvalue with indefinite weight and robin conditions. Calc Var Partial Differ Equ 55(6):1–37. https://doi.org/10.1007/s00526-016-1084-6

Lê A (2006) Eigenvalue problems for the p-Laplacian. Nonlinear Anal: Theory Methods Appl 64(5):1057–1099. https://doi.org/10.1016/j.na.2005.05.056

Liang S, Lou Y (2012) On the dependence of population size upon random dispersal rate. Discrete Contin Dyn Syst B 17(8):2771–2788

Lieb EH, Loss M (2001) Analysis, vol 14. American Mathematical Soc, Providence, RI

Lou Y (2006) On the effects of migration and spatial heterogeneity on single and multiple species. J Differ Equ 223(2):400–426. https://doi.org/10.1016/j.jde.2005.05.010

Lou Y (2008) Some challenging mathematical problems in evolution of dispersal and population dynamics. In: Friedman A (ed) Tutorials in mathematical biosciences IV. Lecture Notes in Mathematics. Springer, Berlin, pp 171–205. https://doi.org/10.1007/978-3-540-74331-6_5

Lou Y, Yanagida E (2006) Minimization of the principal eigenvalue for an elliptic boundary value problem with indefinite weight, and applications to population dynamics. Jpn J Ind Appl Math 23(3):275–292. https://doi.org/10.1007/BF03167595

Mazari I, Ruiz-Balet D (2021) A fragmentation phenomenon for a nonenergetic optimal control problem: optimization of the total population size in logistic diffusive models. SIAM J Appl Math 81(1):153–172. https://doi.org/10.1137/20M132818X

Mazari I, Nadin G, Privat Y (2020) Optimal location of resources maximizing the total population size in logistic models. Journal de mathématiques pures et appliquées 134:1–35. https://doi.org/10.1016/j.matpur.2019.10.008

Mazari I, Nadin G, Privat Y (2021) Optimisation of the total population size for logistic diffusive equations: bang-bang property and fragmentation rate. Commun Partial Differ Equ. https://doi.org/10.1080/03605302.2021.2007533

Nagahara K, Yanagida E (2018) Maximization of the total population in a reaction–diffusion model with logistic growth. Calc Var Partial Differ Equ 57(3):80. https://doi.org/10.1007/s00526-018-1353-7

Skellam JG (1951) Random dispersal in theoretical populations. Biometrika 38(1/2):196–218. https://doi.org/10.1093/biomet/38.1-2.196

Sperner E (1981) Spherical symmetrization and eigenvalue estimates. Math Z 176:75–86. https://doi.org/10.1007/BF01258906

Yousefnezhad M, Mohammadi S (2016) Stability of a predator–prey system with prey taxis in a general class of functional responses. Acta Math Sci 36(1):62–72. https://doi.org/10.21136/AM.2018.0227-17

Yousefnezhad M, Mohammadi SA, Bozorgnia F (2018) A free boundary problem for a predator–prey model with nonlinear prey-taxis. Appl Math 63(2):125–147. https://doi.org/10.21136/AM.2018.0227-17